

# Relationship between surface order and surface azimuthal anchoring strength of nematic liquid crystals

Shinichiro Oka,\* Takashi Mitsumoto, Munehiro Kimura, and Tadashi Akahane

*Department of Electrical Engineering, Faculty of Engineering, Nagaoka University of Technology, 1603-1 Kamitomioka, Nagaoka, Niigata 940-2188, Japan*

(Received 8 December 2003; published 10 June 2004)

The liquid-crystal molecular order near the rubbed polymer surface is reexamined by the improved torque balance method. The surface azimuthal anchoring strength measured by the improved torque balance method is several times larger than that believed conventionally, considered to be significantly affected by the phase-transition behavior. Based on this result, it can be argued that the correlation between the rubbing strength and the surface azimuthal anchoring strength should be improved in consideration of the mechanism of surface order.

DOI: 10.1103/PhysRevE.69.061711

PACS number(s): 61.30.-v, 64.70.Md

## I. INTRODUCTION

The technique of liquid-crystal (LC) alignment is an important issue in the fabrication of liquid-crystal displays (LCD's). Among the many techniques proposed for LC alignment, the rubbing method is at present the most widely used in industry. The rubbing method involves rubbing the polymer-coated substrate surface against a cloth, and despite being a somewhat antiquated technique, the detailed mechanism of LC alignment by the rubbing process has yet to be reported. Recently, the alignment mechanism has been reported to be the result of geometric effects of structures such as grooves [1–5] or a uniaxial expanding effect of the polymer film [6–10]. Although uniform LC alignment can be readily achieved by the rubbing method, the method does present a number of problems, including the generation of dust and static electricity.

A range of alignment techniques have been proposed as potential replacements of the rubbing method, including photoalignment [11], oblique evaporation [12], and a polyimide Langmuir-Blodgett (LB) film method [13]. The photoalignment method is particularly promising as a next-generation method. However, photoalignment is thought to provide only weak anchoring strength with zero pretilt angle at the substrate surface.

In recent years, many types of LCD's have been proposed and developed, and these displays have become very popular in a range of applications such as cellular phones, personal computers, and televisions. In the fabrication of LCD's, the quality of surface treatment is very important, as factors such as anchoring strength and pretilt angle affect the image quality and the driving characteristics. Hence, extensive research has been conducted on methods of surface treatment.

In 1979, Miyano showed that wall-induced pretransitional birefringence is a valuable phenomenon for studying the orienting forces of LC molecules [7,14]. In particular, wall-induced pretransitional birefringence indicates the orientational order parameter at the boundary, and can be measured

in the isotropic phase. This birefringence is sensitive only to the short-range force.

Several methods for measuring the surface azimuthal anchoring strength have been proposed, including the Néel wall method [15,16], the torsional torque balance method [17,18], and the improved torque balance method [19]. It has been shown that the resultant surface azimuthal anchoring strength measured by the conventional torque balance method and the improved torque balance method differs for an LCD consisting of the liquid-crystal MLC-2051 (Merck) and the alignment film PVCi (polyvinyl cinnamate) [19]. It is thought that this discrepancy is due to the adsorption of liquid-crystal molecules on the alignment film.

In this study, the relationship between the surface order and the surface azimuthal anchoring strength of the nematic LC is examined in detail. The surface azimuthal anchoring strength is measured using both the conventional torque balance method and the improved torque balance method, and the relationship between the surface azimuthal anchoring strength, surface order, and phase-transition characteristics is discussed. The surface azimuthal anchoring strength is reexamined in light of the present results, and an appropriate measurement method is proposed from a physical viewpoint.

## II. EXPERIMENT

Two alignment films, polyvinyl alcohol (PVA) and polyimide (PI), were applied to glass substrates. The pretilt angles generated by the rubbing method were approximately 0° and 4° for PVA and PI, respectively, measured by the crystal rotation method [20]. Surface alignment was performed by the rubbing method in order to make TN cells and antiparallel homogeneous cells. Uchida *et al.* showed that the relationship between the surface azimuthal anchoring strength and the rubbing strength can be defined in terms of a rubbing strength parameter [21,22]. The rubbing strength  $L$  (mm) is given by

$$L = Nl \left( 1 + \frac{2\pi r n}{60v} \right), \quad (1)$$

where  $N$  is the cumulative number of rubbing passes,  $l$  (mm) is the contact length of the circumference of the rubbing

\*Electronic address: shioka@gm.hrl.hitachi.co.jp

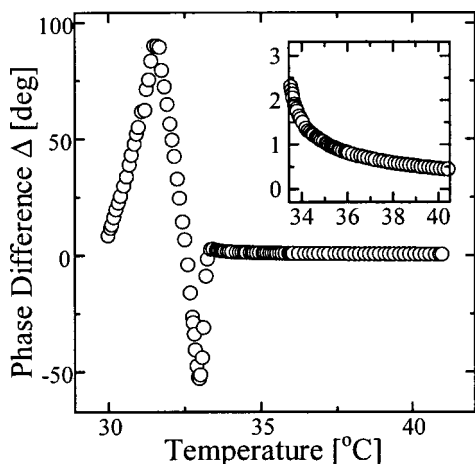


FIG. 1. Dependence of LC cell retardation on temperature around the N-I transition for PVA and 5CB. (Inset) Magnification of the region near the phase-transition temperature.

roller;  $n$  (rpm) is the rate of roller rotation,  $r$  (mm) is the roller radius, and  $v$  (mm/s) is the velocity of the substrate stage. Beads of 5- $\mu\text{m}$  diam were used as spacers. The LC substances used in this study were 4-cyano-4'- $n$ -pentylbiphenyl (5CB) ( $T_c=35.5^\circ\text{C}$ ), MLC-2051 ( $T_c=68.0^\circ\text{C}$ ), and ZLI-4792 ( $T_c=92.0^\circ\text{C}$ ), all supplied by Merck Co. Ltd. The LC was injected into the cell in the isotropic phase by capillary action. The behavior of the surface LC on the alignment film was observed in three experiments. First, the phase-transition behavior was observed under an optical polarization microscope. This technique visualizes the transformation of the LC from the isotropic phase to the nematic phase, the characteristics of which vary depending on the type of LC and alignment treatment [24]. In the case of bulk transition, as the temperature decreases from the isotropic phase, the nematic phase appears as circular domains of size equivalent to the thickness of the LC cell. In the case of surface transition, however, the field of view becomes gradually brighter as a result of pretransitional behavior, followed by the uniform appearance of the nematic

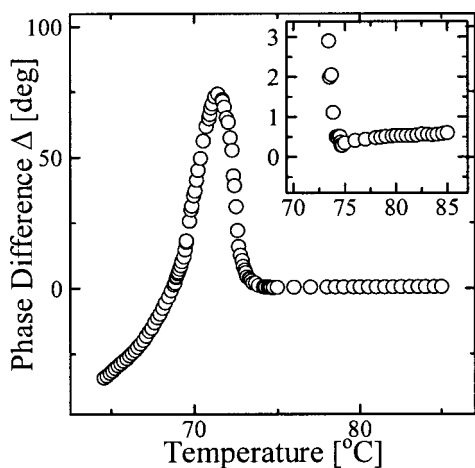


FIG. 2. Dependence of LC cell retardation on temperature around the N-I transition for PVA and MLC-2051. (Inset) Magnification of the region near the phase-transition temperature.

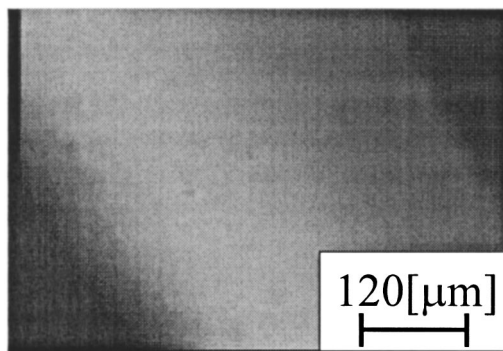


FIG. 3. Polarizing micrograph of the N-I transition in a cell with PVA and 5CB.

phase. It is thought that the characteristic phase-transition behavior depends on the wettability between the LC and the alignment film in the nematic phase, as well as the surface order [25].

Second, the surface azimuthal anchoring strength was measured by the conventional torque balance method and the improved torque balance method. In the case of the conventional torque balance method, the surface azimuthal anchoring strength can be calculated from the director's twist angle of the TN cell. For measurement by the improved torque balance method, the initial sample setup should be a homogeneous cell rather than a TN cell. A spatially uniform planar cell was cooled below the IN transition, allowing the molecules at the surface to align along easy axes. After three days, one substrate was rotated by  $90^\circ$  and the rotation angle of the liquid crystal was measured. Here, the twist angle of the TN cell was measured using a polarization-modulated spectroscopic ellipsometer (PMSE) (M-150, Jasco). The actual thickness of the LC layer was determined by ellipsometry at the same time [23]. It has already been confirmed that the twist angle and cell gap measured by this method incur an error of less than 0.1% when the pretilt angle at the substrate surface is less than  $5^\circ$ . The pretilt angle of the PI surface was neglected in the present experiments. Using the experimental results, the surface azimuthal anchoring strength  $A_\phi$  is given by

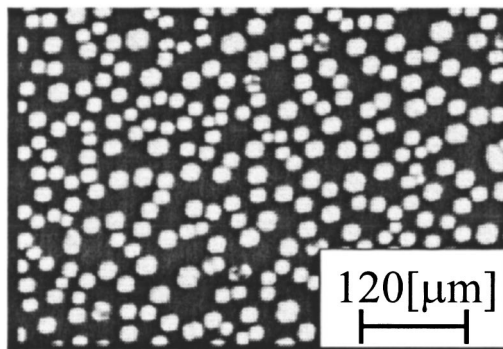


FIG. 4. Polarizing micrograph of the N-I transition in a cell with PVA and MLC-2051.

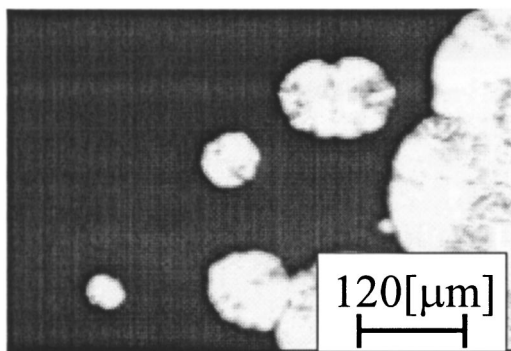


FIG. 5. Polarizing micrograph of the N-I transition in a cell with PVA (unrubbed) and 5CB.

$$A_{\phi} = \frac{2K_{22}\Phi_t}{d \sin 2\Delta\Phi}, \quad (2)$$

where  $K_{22}$  is the twist elastic constant,  $d$  is the actual thickness of the LC layer, and  $\Phi_t$  is the actual twist angle of the director throughout the cell.  $\Delta\Phi$  is given by

$$2\Delta\Phi = \Phi_t^0 - \Phi_t, \quad (3)$$

where  $\Phi_t^0$  is the angle between the easy axes of the substrates. 5CB and MLC-2051 have  $K_{22}$  values of 5.50 and 4.09 pN, respectively.

Finally, the surface order was evaluated by measuring the remnant order at the surface in the isotropic phase. In a perfectly isotropic condensed phase, the optical retardation should be zero. However, the retardation of the LC cell is not zero even when the LC is in the isotropic phase, and the greater the retardation of the LC cell in the isotropic phase, the higher the order parameter at the surface. This is called wall-induced pretransitional birefringence, and is usually measured using an ellipsometer with an He-Ne laser.

Figures 1 and 2 show example results for the temperature dependence of retardation near the nematic-isotropic N-I transition temperature for PVA alignment film and a rubbing strength  $L$  of 2146 mm. The LC's used in these cases were 5CB (Fig. 1) and MLC-2051 (Fig. 2). The phase-transition temperatures of 5CB and MLO-2051 in this study were 33.0 and 74.0°C, respectively. Wall-induced pretransitional bire-

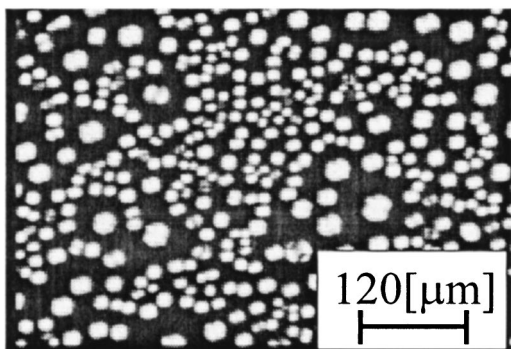


FIG. 6. Polarizing micrograph of the N-I transition in a cell with PVA (unrubbed) and MLC-2051.

TABLE I. Behavior of isotropic-nematic phase transition with and without rubbing (alignment) treatment.

LC	Rubbed	Unrubbed
5CB	Surface transition	Surface transition
MLC-2051	Bulk transition	Bulk transition
ZLI-4792	Surface transition	Bulk transition

fringence was observed in both experiments, with different results for the measured absolute birefringence. In this paper, the retardation measured in this temperature range is referred to as the residual retardation. From preliminary experiments, the temperature adopted for measurement of the residual retardation was set at 36.5°C for 5CB and 77.0°C for MLC-2051.

### III. RESULTS AND DISCUSSION

Figures 3 and 4 show polarizing micrographs of the phase transition in the 5CB and MLC-2501 cells with PVA alignment film after rubbing with a cotton cloth. The difference in the behavior of the phase transition can be easily recognized in this figure. In the case of 5CB, as the temperature decreases from the isotropic phase, the boundary line between the nematic phase and the isotropic phase moves at a constant speed until the entire region reaches the nematic phase, indicating that the transition begins in the vicinity of the substrate. In contrast, for MLC-2051, nematic droplets form sporadically as the temperature of the LC sample decreases below the phase-transition temperature. These droplets gradually become larger, eventually merging and coming to occupy the entire region and complete the transition. This behavior indicates that the transition begins in the LC bulk. It is thought that the wettability between the LC and the alignment film is relatively high in the former case, while in the latter case the wettability is relatively low and/or the bulk transition temperature is different from the surface transition

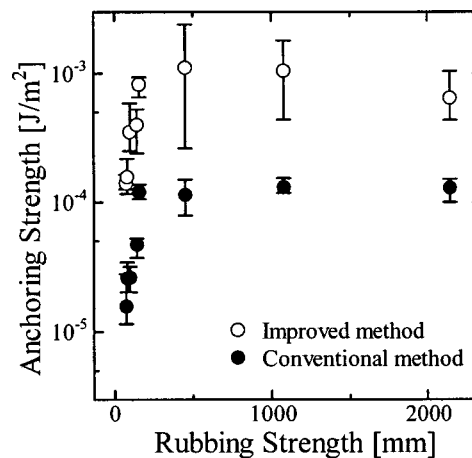


FIG. 7. Surface azimuthal anchoring strength measured by the improved torque balance method (open circles) and the conventional torque balance method (closed circles) as a function of rubbing strength for 5CB and PVA.

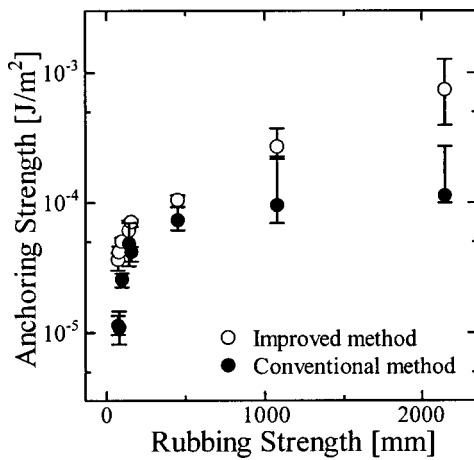


FIG. 8. Surface azimuthal anchoring strength measured by the improved torque balance method (open circles) and the conventional torque balance method (closed circles) as a function of rubbing strength for 5CB and PI.

temperature since the MLC-2051 is a mixture of LC's.

Figures 5 and 6 show photographs of the phase transition for 5CB and the MLC-2501 with unrubbed (unaligned) PVA film. Although no alignment treatment was applied to the PVA, the behavior of the transition is similar to the case for the rubbed substrates. ZLI-4792, however, exhibited different transition behavior depending on the alignment of the substrate. The observed phase-transition behaviors are summarized in Table I. These experimental results imply that the behavior of the transition is determined by the type of LC and alignment film and alignment treatment.

Figures 7 and 8 show the dependence of the surface azimuthal anchoring strength measured by the conventional torque balance method and the improved torque balance method on the rubbing strength. These results were obtained for 5CB as the LC and for PVA and PI as the alignment film. The surface azimuthal anchoring strength measured by both methods varies with the rubbing strength, but that measured by the improved torque balance method is significantly higher. This difference is interpreted as being related to the

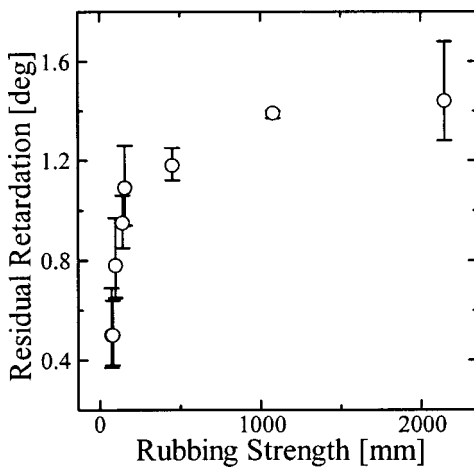


FIG. 9. Residual retardation vs rubbing strength for 5CB and PVA.

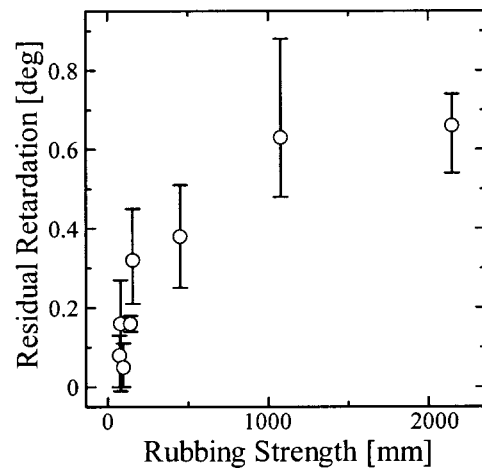


FIG. 10. Residual retardation vs rubbing strength for 5CB and PI.

residual retardation. Figures 9 and 10 shows the rubbing strength versus the residual retardation of 5CB measured under the same conditions as for Figs. 7 and 8. These results demonstrate that there is a relationship between the residual retardation and the measured surface azimuthal anchoring strength.

Figures 11 and 12 show the dependence of the surface azimuthal anchoring strength on rubbing strength for MLC-2051 with PVA and PI alignment films, respectively. Measurements were made under the same conditions as for Figs. 7 and 8. The anchoring strength measured by the conventional torque balance method varies with rubbing strength in a similar manner to Figs. 7 and 8. However, the surface azimuthal anchoring strength measured by the improved torque balance method does not exhibit such a strong dependence on the rubbing strength. Figures 13 and 14 show rubbing strength versus residual retardation for MLC-2051 and 5CB. Only the residual retardation of MLC-2051 exhibits a dependence on the rubbing strength.

Figures 15 and 16 show the relationship between the residual retardation and azimuthal anchoring strength for 5CB

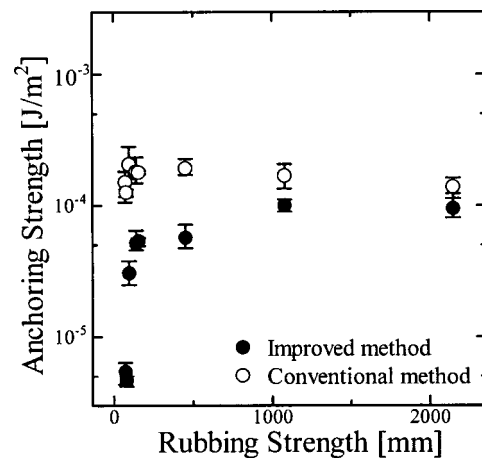


FIG. 11. Surface azimuthal anchoring strength measured by the improved torque balance method (open circles) and the conventional torque balance method (closed circles) as a function of rubbing strength for MLC-2051 and PVA.

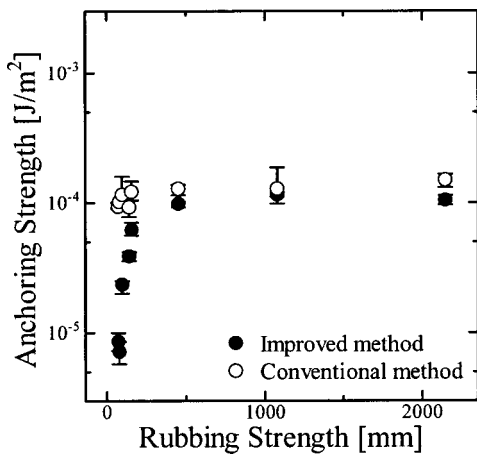


FIG. 12. Surface azimuthal anchoring strength measured by the improved torque balance method (open circles) and the conventional torque balance method (closed circles) as a function of rubbing strength for MLC-2051 and PI.

with PVA and PI alignment films, respectively, measured by the improved torque balance method. Figures 17 and 18 show the relationship between the residual retardation and azimuthal anchoring strength for MLC-2051 with PVA and PI alignment films, respectively, measured by the improved torque balance method. It was easily recognized that the behavior of the azimuthal anchoring strength is a significant difference between the 5CB and the MLC-2051. In the case of the 5CB, the azimuthal anchoring strength depends strongly on the residual retardation, while in the case of the MLC-2051, the azimuthal anchoring strength does not depend on the residual retardation.

In all of these experiments, the surface azimuthal anchoring strength measured by the improved torque balance method is higher than that measured by the conventional torque balance method. As described in the previous paper [19], the improved torque balance method provides a more accurate measurement of the azimuthal anchoring strength in line with the true physical definition, taking the adsorption effect of the surface into consideration. In case of the

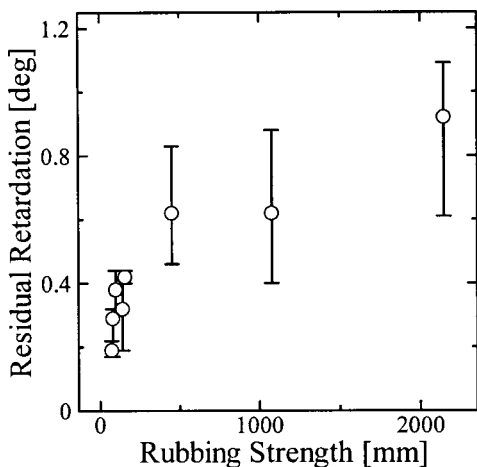


FIG. 13. Residual retardation vs rubbing strength for MLC-2051 and PVA.

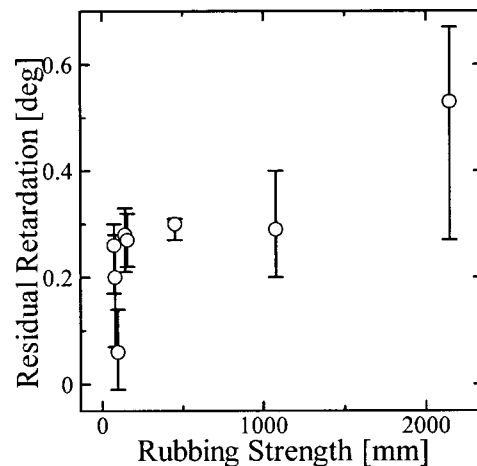


FIG. 14. Residual retardation vs rubbing strength for was 5CB and PI.

surface-type LC transition, the alignment of the LC molecules is memorized at the substrate surface when the temperature of the LC cell cools down from the isotropic phase to the nematic phase, aligning the easy axis parallel with the rubbing direction. However, in the case of the bulk transition, the LC molecules of the TN cell are not adsorbed onto the substrate surface. After the LC molecules in the bulk have completed the transition to the nematic phase, the surface LC becomes adsorbed onto the alignment film and elastic torque from the bulk causes the alignment axis to deviate from the rubbing direction. This behavior therefore indicates a deviation of the easy axis [26]. However, it is thought that LC transition behavior is determined by both the wettability and the surface order induced by alignment treatment. Hence, the surface azimuthal anchoring strength measured by the conventional torque balance method in fact reflects the dependence on the residual retardation and/or rubbing strength.

The present results obtained by the improved torque balance method show that the adsorption of 5CB is stronger than for MLC-2051, and that the surface azimuthal anchor-

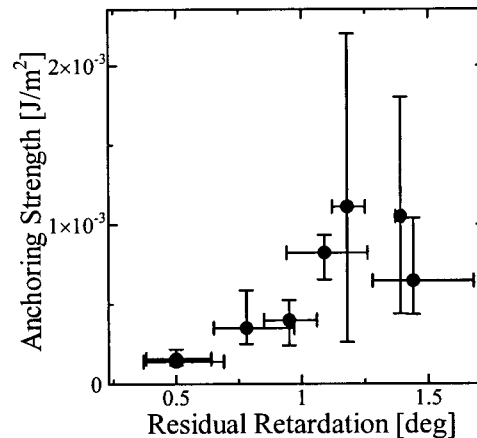


FIG. 15. Azimuthal anchoring strength measured by the improved torque balance method vs the residual retardation for 5CB and PVA.

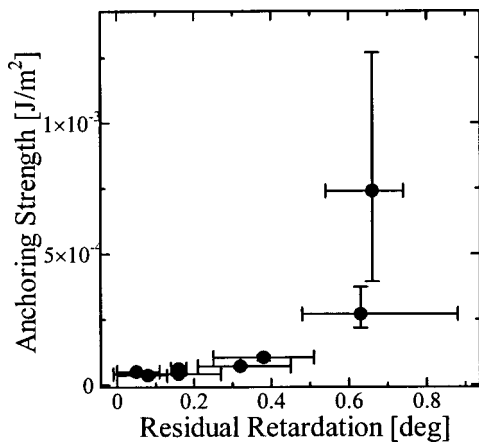


FIG. 16. Azimuthal anchoring strength measured by the improved torque balance method vs the residual retardation for 5CB and PI.

ing strength of 5CB is dependent on the rubbing strength dependence whereas that for MLC-2051 is not. This is considered to be due directly to the difference in I-N phase transition behavior, as described schematically in Fig. 19. When an ordered nematic layer is formed in the vicinity of the alignment film surface at temperatures near the N-I transition point, as is the case for 5CB, it is natural that the order parameter of the surface nematic LC layer depends on the surface anisotropy of the rubbed alignment film. As a result, the surface azimuthal anchoring strength depends on the rubbing strength. In contrast, a lack of wettability between the LC and the alignment film, as seen for MLC-2051, prevents the formation of such an ordered nematic layer in the vicinity of the alignment film, even at temperatures below the N-I transition point. After the nematic droplets grow and finally contact the alignment film surface, the interface between the nematic layer and the alignment film is formed. In this case, the azimuthal anchoring strength is strongly affected by the bulk order, while the surface anisotropy of the alignment film may have a small influence on the azimuthal anchoring strength. Therefore, it seems that the surface azimuthal an-

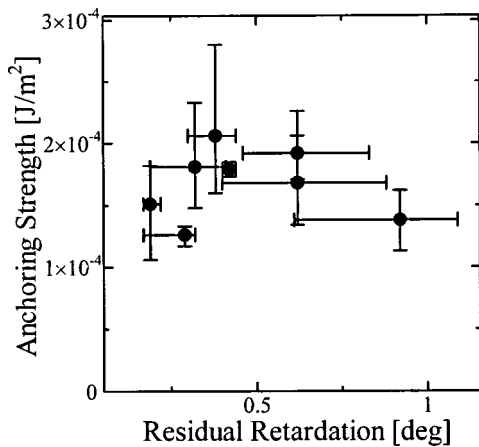


FIG. 17. Azimuthal anchoring strength measured by the improved torque balance method vs the residual retardation for MLC-2051 and PVA.

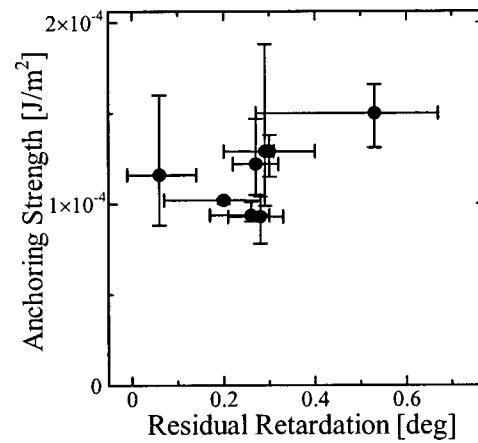


FIG. 18. Azimuthal anchoring strength measured by the improved torque balance method vs the residual retardation for MLC-2051 and PI.

choring strength does not depend on the rubbing strength for these types of LC's; only the residual retardation is dependent on the rubbing strength. The transition behavior itself appears to be determined by the wettability of the nematic LC and the surface order.

Consequently, even though the same alignment film may be used, the effect of the rubbing strength on the surface azimuthal anchoring strength depends on the type of LC. The present findings also reiterate that the conventional torque balance method and the Néel wall method, etc., are not applicable for measurement of the surface azimuthal anchoring strength. Any method for measuring the surface azimuthal anchoring strength accurately must consider the importance of adsorption, as do the improved torque balance method and the alignment transcription method [27].

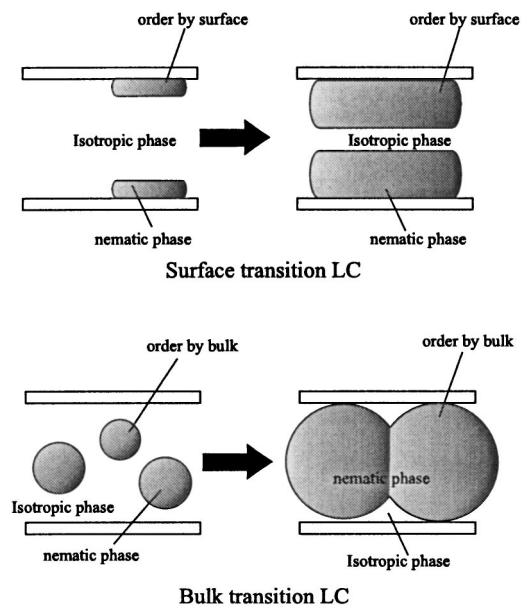


FIG. 19. Two modes of transition from isotropic to nematic LC.

#### IV. CONCLUSIONS

Experiments and discussion on the isotropic-nematic phase-transition behavior provided a clear interpretation of the relationship between the surface order and the surface azimuthal anchoring strength. The results confirm the inadequacy of the conventional torque balance method for measurement of the surface azimuthal anchoring strength, and demonstrate the necessity of understanding the behavior of

polymer films and the effect of surface treatments such as rubbing. It was shown to be important to consider not only the surface wettability on the alignment films but also the surface order formed by surface treatment. Most importantly, however, the present experiments clearly demonstrated that the characteristics of both the alignment film and the liquid crystal should be taken into consideration in developing and tuning LC fabrication processes.

- 
- [1] D. W. Berreman, *Phys. Rev. Lett.* **28**, 1683 (1972).  
 [2] D. W. Berreman, *Mol. Cryst. Liq. Cryst.* **23**, 215 (1973).  
 [3] U. Wolff, W. Grenbel, and H. Kruger, *Mol. Cryst. Liq. Cryst.* **23**, 187 (1973).  
 [4] L. T. Creagh and A. R. Kmetz, *Mol. Cryst. Liq. Cryst.* **24**, 59 (1973).  
 [5] M. Nakamura, *J. Appl. Phys.* **52**, 4561 (1981).  
 [6] J. Dubois, M. Gazard, and A. Zann, *J. Appl. Phys.* **47**, 1270 (1975).  
 [7] K. Miyano, *Phys. Rev. Lett.* **43**, 51 (1979).  
 [8] J. M. Geary, J. W. Goodby, A. R. Kmetz, and J. S. Patel, *J. Appl. Phys.* **62**, 4100 (1987).  
 [9] S. Ishihara, H. Wakemoto, K. Nakazima, and Y. Matsuo, *Liq. Cryst.* **4**, 669 (1989).  
 [10] K. Nakajima, H. Wakemoto, S. Sato, F. Yokotani, S. Ishihara, and Y. Matsuo, *Mol. Cryst. Liq. Cryst.* **180**, 223 (1990).  
 [11] M. Schadt, K. Schmitt, V. Kozinkov, and V. Chigrinov, *Jpn. J. Appl. Phys., Part 1* **31**, 2155 (1992).  
 [12] T. Uemura, N. Ohba, H. Ohnishi, and I. Ota, *Proc. SID'86* (Society for Information Display, New York, 1987), Vol. 28-2, p. 175.  
 [13] H. Ikeno, A. Oh-saki, N. Ozaki, M. Nitta, K. Nakaya, and S. Kobayashi, *SID'88 Digest*, 45 (1988).  
 [14] K. Miyano, *J. Chem. Phys.* **71**, 4108 (1979).  
 [15] G. Ryschenkow and M. Kleman, *J. Chem. Phys.* **64**, 404 (1976).  
 [16] Y. Iimura, S. Kobayashi, T. Hashimoto, T. Sugiyama, and K. Katoh, *IEICE Trans. Electron.* **E79-C**, 1040 (1996).  
 [17] Y. Iimura, N. Kobayashi, and S. Kobayashi, *Jpn. J. Appl. Phys., Part 2* **33**, L189 (1994).  
 [18] T. Akahane, H. Kaneko, and M. Kimura, *Jpn. J. Appl. Phys., Part 1* **35**, 4434 (1996).  
 [19] K. Okubo, M. Kimura, and T. Akahane, *Jpn. J. Appl. Phys., Part 1* **42**, 6428 (2003).  
 [20] T. J. Scheffer and J. Nehring, *J. Appl. Phys.* **48**, 1783 (1977).  
 [21] T. Uchida, M. Hirono, and H. Sakai, *Liq. Cryst.* **5**, 1127 (1989).  
 [22] Y. Sato, K. Sato, and T. Uchida, *Jpn. J. Appl. Phys., Part 2* **31**, L579 (1992).  
 [23] M. Kimura, S. Okutani, H. Toriumi, K. Akao, T. Tadokoro, and T. Akahane, *Mol. Cryst. Liq. Cryst. Sci. Technol., Sect. A* **367**, 691 (2001).  
 [24] H. Yokoyama, S. Kobayashi, and H. Kamei, *Mol. Cryst. Liq. Cryst.* **99**, 39 (1983).  
 [25] H. Yokoyama, S. Kobayashi, and H. Kamei, *J. Appl. Phys.* **56**, 2645 (1984).  
 [26] H. Akiyama and Y. Iimura, *Jpn. J. Appl. Phys., Part 2* **41**, L521 (2002).  
 [27] Y. Toko, B.-Y. Zhang, T. Sugiyama, K. Katoh, and T. Akahane, *Mol. Cryst. Liq. Cryst. Sci. Technol., Sect. A* **304**, 107 (1997).